GEOPHYSICAL RESEARCH LETTERS, VOL. 23, 6, DOI:10.1029/96GL00453, MARCH 1996

Whistler waves in 3D hybrid simulations of quasiperpendicular shocks

P. Hellinger[1,3], A. Mangeney[1], A. Matthews[2]

We investigate a low Mach number supercritical quasiperpendicular shock using a three-dimensional hybrid code. We find an out-of-coplanarity whistler wave mode propagating upstream, with properties similar to those of the "upstream whistlers" observed in the vicinity of planetary shocks. We discuss the generation mechanism, which turns out to be driven by the free energy provided by reflected protons.

1. Introduction

Whistler mode waves are a common feature of the wave turbulence in the upstream region of collisionless shocks, and they have been repeatedly observed upstream of planetary bow shocks [for example *Fairfield*, 1974; *Orlowski and Russell*, 1991]. We shall be concerned here with the so called "1 Hz whistlers" or "upstream whistlers" which are most easily observed beyond the shock foot [for example *Orlowski et al.*, 1994].

The mechanism by which they are generated is not yet understood; several possibilities have been proposed: generation within the shock ramp by some instability involving the particles reflected by the shock, [for example *Tokar and Gurnett*, 1985], by nonlinear dispersive effects [*Galeev et al.*, 1988] or generation upstream of the shock by a beam type instability [*Wong and Goldstein*, 1988; *Gurgiolo et al.*, 1993].

We consider here the case of a weakly supercritical quasiperpendicular shock for which whistler waves with properties similar to those observed happen to be most easily identifiable.

2. Simulation model and shock parameters

We use a 3D version of the hybrid code which has been described in *Matthews* [1994].

Fields and momenta are defined on a 3D grid with dimensions $n_x \times n_y \times n_z = 200 \times 20 \times 40$, where x is the shock normal direction. The spatial resolution is $dx = dz = 0.125c/\omega_{pi}$, $dy = 0.25c/\omega_{pi}$, where c is the speed of light and ω_{pi} the upstream proton plasma frequency. There are 15 particles per cell in the region upstream of the shock and the time step for the particle advance is $dt = 0.05\Omega_i^{-1}$ (Ω_i: upstream proton gyrofrequency), while the magnetic field **B** is advanced with a smaller time step $dt_B = dt/20$.

The code, in its 1D version, has been tested in particular for the propagation of small amplitude magnetosonic waves. The numerical dispersion relation agrees with the theoretical one up to frequencies as high as $30-40\Omega_i$.

The shock is launched in the standard way by reflection of a streaming plasma on an infinitely conducting wall. The parameters of the simulation are: plasma injection velocity, $v_0 = 2v_A$, directed parallel to the x axis, angle between the shock normal and the upstream magnetic field vector (in the coplanarity plane xz), $\theta_{Bn} = 80^\circ$, the proton and electron pressures normalized to the upstream magnetic pressure, $\beta_p = \beta_e = 0.5$, and resistivity, $\eta = 10^{-3}\mu_0 v_A^2/\Omega_i$ (v_A is the upstream Alfvén speed and μ_0 is the permeability of vacuum). A typical particle will then cross a cell in $1.25dt$; we checked that the results do not depend on the time step by comparing with a simulation using a smaller time step $dt = 0.025\Omega_i^{-1}$.

These plasma parameters lead to the formation of a slightly supercritical shock with an Alfvén Mach number $M_A \simeq 3.3$ travelling in the direction of decreasing x.

3. Simulation results

In the vicinity of the shock we observe the usual population of reflected particles which do not escape upstream, but are transmitted downstream [see for example *Burgess*, 1987]. In high Mach number ($M_A \geq 4-5$) simulations, the fluctuations in the vicinity of the shock ramp are dominated by Alfven ion cyclotron (AIC) waves [*Winske and Quest*, 1988; *Thomas*, 1989]. Actually we observe that these waves are not excited when the Alfven Mach number is smaller than $4-5$ (the reason seams to be that the convective time is less then the instability time but a further investigation is beyond the scope of this paper and will be treated elsewhere). This is the case we are considering here.

Figure 2 shows profiles of the averaged density and of the relative fluctuations of the density and of the magnetic field amplitude. These fluctuations cover a frequency range (in the simulation frame) of $[1-20]\Omega_i$ (such high frequencies are allowed by the field substepping mentionned above).

The maximum amplitude of the magnetic field fluctuation, $\delta B/B \sim 1$, and of the density fluctuations, $\delta\rho/\rho \sim 0.4$, is reached in the ramp region ($11c/\omega_{pi} < x < 12c/\omega_{pi}$) where the reflected proton density represents roughly $5-10\%$ of the incident bulk flow density. The existence of such strong fluctuations is explained by the presence of an out of coplanarity wave mode which is clearly visible in figure 3. This figure shows two $2D$ cuts of the z-component B_z of the magnetic field in a coplanarity plane and in a shock plane (located at the front of the shock, $x = 11.25c/\omega_{pi}$). The mode amplitude is concentrated in the region $9c/\omega_{pi} < x < 12c/\omega_{pi}$ covering the shock ramp and the foot. Using a 3D Fourier analysis we estimate the wavelength $\lambda \simeq 1c/\omega_{pi}$, the angles between the wave vector and the mean magnetic field: $\theta_{kB} \simeq 131^\circ$, the shock normal: $\theta_{kn} \simeq 51^\circ$, the coplanarity plane: $\theta_{kc} \simeq 56\,\mathrm{deg}$.

In the plasma frame the mode is elliptically polarized in the right handed sense, its frequency is $\omega \simeq 27\Omega_i$ and phase speed is $v_{ph} \simeq 5.1v_A$ directed upstream, in agreement with the characteristics of the high frequency right handed branch of the fast magnetosonic mode (which we will call a whistler as usual in space plasma physics). Using WHAMP [*Rönmark*, 1982] we obtained the corresponding dispersion relation for a homogeneous hot Maxwellian plasma, displayed in figure 4; in the $(\omega - k)$ plane the mode identified in the simulation (denoted by an asterisk) falls close to the theoretical curve.

The linear analysis predicts also that the wave has an electromagnetic character and a compressibility ratio $(\delta\rho/\rho_0)/(\delta B_z/B_0) \sim$

[1]Observatory of Paris, Meudon, France
[2]Departement of Physics, University of Natal, Durban, South Africa
[3]Now at Institute of Atmospheric Physics, Prague, Czech Republic

0094-8276/04/96GL00453$5.00

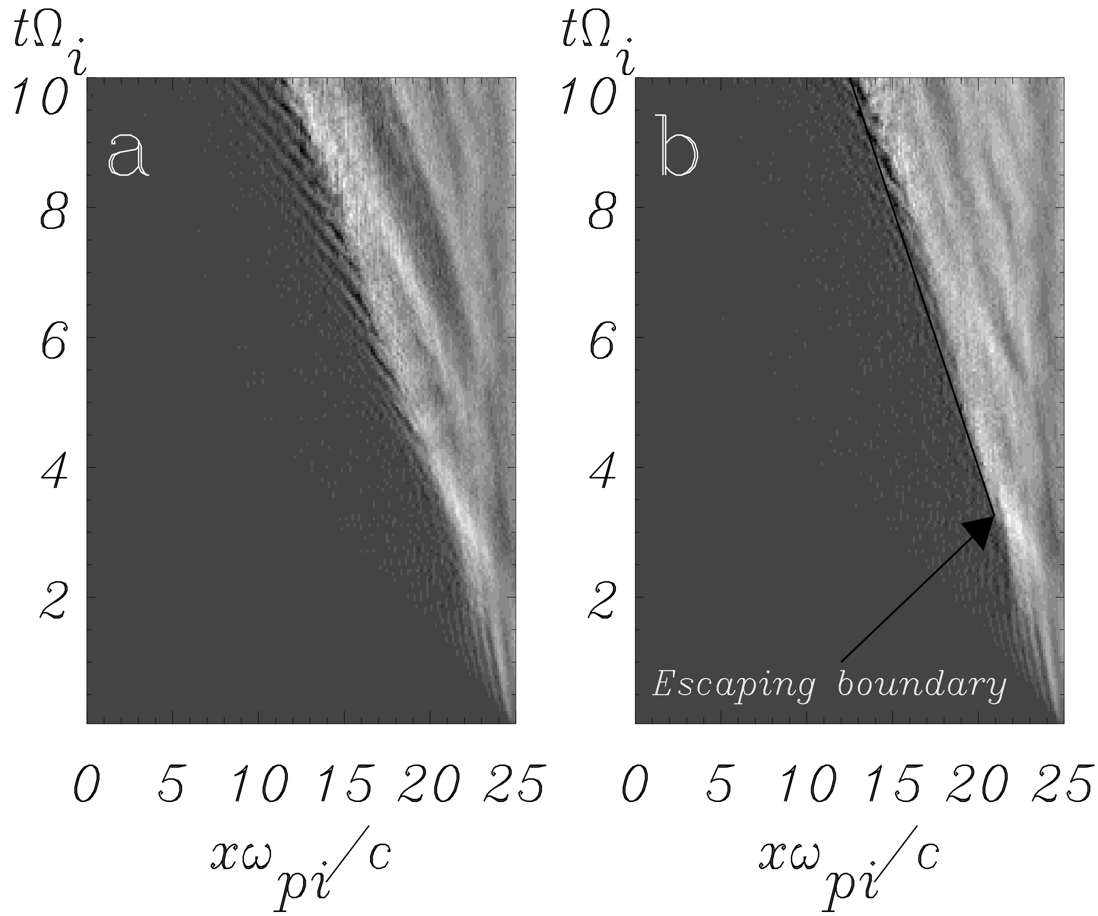

Figure 1. Time evolution of B_z in the case with reflected protons (a) and in the case where reflected protons are removed upstream of a moving escaping boundary (b).

$5 \cdot 10^{-2}$. This is only partly in agreement with the simulation result, where the mode has a rather strong longitudinal electric field component $E_\parallel \sim E_\perp$ ($E_\parallel = |\mathbf{k} \cdot \mathbf{E}|/k$, $E_\perp = |\mathbf{k} \times \mathbf{E}|/k$). It is also apparent in figure 2 that the density fluctuation in the ramp is much higher than expected from the linear analysis. Moreover the phase shift between δB and $\delta\rho$ in this region varies between $\pi/2$ and $3\pi/2$. These results are not consistent with the linear analysis; the density fluctuation connected with the wave is either a quasilinear effect or is a consequence of the strong gradients in the front of the shock.

As seen in figure 1a which displays in grey levels the amplitude of B_z in a (x, t) plane, at y, z fixed, the waves penetrate in the upstream plasma with a group velocity $v_{gx} \simeq -5.$ somewhat faster than the shock, but consistent with the estimate from the linear theory. The damping is negligible, the resistive damping length being larger than the box dimensions.

4. Generation mechanism

The instability of a gyrotropic gyrating beam, studied by *Wong and Goldstein* [1988], appears to be a good candidate for the excitation of the observed whistlers. Indeed, the waves which are destabilized by this instability belong also to the high frequency ($\omega > 10\Omega_i$), right handed elliptically polarized branch of the fast magnetosonic mode. The instability is resonant and the most unstable wave vectors $\mathbf{k}$ lie in the plane containing the directions of the magnetic field $\mathbf{B}$ and of the beam velocity $\mathbf{v}_b$ but are not aligned with either directions when the angle between $\mathbf{B}$ and $\mathbf{v}_b$ is sufficiently large.

These properties are consistent with those of the whistlers observed in the simulation. The wavelength, frequency and polarisation are just what can be expected; furthermore the wave vector satisfies approximatively $\mathbf{k}\cdot(\mathbf{B}\times\mathbf{v}_b) \simeq 0$ and the resonance condition in the plasma frame, $\mathbf{k}\cdot\mathbf{v}_b \simeq 26 \simeq \omega$ (we have used here the upstream magnetic field, the wave vector given above and an average value for the reflected beam velocity $\mathbf{v}_b \simeq (-3., 3.6, 0.)$ calculated in the interval $9c/\omega_{pi} < x < 11c/\omega_{pi}$).

A comparison with a simulation having a lower resolution so as to suppress the whistler wave mode shows that the transmitted protons are not heated by the wave while there is some heating of the reflected protons, as expected from quasilinear diffusion of the resonant particles by the unstable waves.

A more detailed comparison between the simulation and the model by *Wong and Goldstein* [1988] is extremely difficult because of the complicated proton distribution functions which characterize the foot and ramp region (in particular the uncertainty on $\mathbf{v}_b$ is relatively large). Moreover the spatial gradients for density and magnetic field, which in the simulations are comparable to the wavelength of the whistler mode, are not included in the spatially uniform model of *Wong and Goldstein* [1988].

In order to investigate further the role of the reflected particles for the generation of the whistlers, we have run the same simulation as described above except that the reflected particles are removed from the simulation at some distance upstream of the shock (the escape boundary). The results of such a simulation are shown in figure 1b where an escape boundary, moving at constant velocity in the simulation frame, precedes the shock throughout the simulation. The presence of the escape boundary modifies the momentum balance of the shock and its velocity so that its distance to the escape boundary changes as a function of time. At times when the escape boundary is close to the shock ramp ($t \sim 4 - 6\Omega_i^{-1}$), no whistlers are present. When the distance between the shock ramp and the escape boundary exceeds some distance the whistlers reappear as in the original simulation (figure 1a).

Note that it is only the most energetic reflected particles, those which can reach the escape boundary, that are removed. The fact that when they are absent the waves disappear suggests that they are responsible for the development of the instability.

5. Conclusion

We have given some evidence that reflected protons can generate whistler mode waves by a gyrating gyrotropic proton beam instability [*Wong and Goldstein*, 1988].

Since the wave amplitude decreases upstream with increasing distance from the shock ramp, the reflected protons excite the waves when they gyrate back into it and not upstream as proposed by *Wong and Goldstein* [1988].

Another alternative explanation could be the nonlinear dispersive generation of whistler waves oblique with respect to the shock normal [*Krasnoselskikh et al.*, 1994], an explanation which cannot be immediately dismissed in the present stage of our investigations. Even the fact that the waves disappear when an escape boundary is imposed for the reflected particles is not really conclusive since the macroscopic structure of the shock is clearly affected by the presence of this escape boundary. Note that dispersive whistlers, which propagate parallel to the shock normal are only visible during the initial phase of the formation of the shock ($t \sim 0 - 2\Omega_i^{-1}$) but they disappear afterwards (see figure 1a).

However the overall agreement between the properties of the waves observed in the simulation with those predicted by the linear theory provides a very strong case in favor of their generation by an instability involving reflected protons. There are still open problems: one is a more quantitative comparison with the linear theory, another is a deeper understanding of the simulation where the reflected particles are removed; these questions are beyond the scope of the present letter and will be investigated elsewhere.

Are the high frequency magnetosonic waves which we observe in the simulation similar to those found in the vicinity of planetary shocks? As discussed above, there are strong similarities in the frequency range and polarisation properties; they also propagate obliquely with respect to the magnetic field and shock normal. However the wave vector of the simulation whistlers makes a finite angle $\theta_{kc} \simeq 56\,\mathrm{deg}$ with the coplanarity plane while in a recent study of upstream whistlers at the Venus bowshock by *Orlowski et al.* [1994], found that the wave vectors are distributed mostly in the coplanarity plane. It is not clear wether this is serious difficulty or not. First it should be noted that the simulation value of θ_{kc} falls at the limit but within the range of observed values. Second, we have considered here a simple but rather special case; indeed the shock is close to being perpendicular; it is expected that for more oblique shocks, where the beam velocity has a significant component along the magnetic field, the most unstable wave vector will come closer to the coplanarity plane. These questions are presently investigated.

A similar mechanism for the generation of oblique whistlers appears to work in the case of higher Mach number shocks. A 2D full particle simulation by *Krauss-Varban et al.* [1995] using a small electron to proton mass ratio obtained similar results for a $60\,\mathrm{deg}$ shock with $M_A = 5$, as far as the upstream whistlers are concerned. In particular the electrons appear unable to provide the free energy for the instability but are responsible for the dissipation mechanism through the Landau damping [see also *Orlowski et al.*, 1995].

It is worthwhile to note that the use of a 3D code has been extremely useful in order to identify the instability mechanism responsible for the generation of the waves. Instability is also allowed in a 2D simulation but it misses one of its most significant signature which is the fact that the most unstable wave vectors belong to the plane containing the directions of the magnetic field and of the beam velocity, at least in the range of parameters considered here.

References

Burgess, D., Simulations of backstreaming ion beams formed at oblique shocks by direct reflection, *Ann. Geophys.*, *5A*, 133–146, 1987.

Fairfield, D. H., Whistler waves observed upstream from collisionless shocks, *J. Geophys. Res.*, *79*, 1368–1378, 1974.

Galeev, A., C. Kennel, V. Krasnoselskikh, and V. Lobzin, The role of whistler oscillations in the formation of the structure of high Mach number collisionless shock, in *Proceedings of Joint Varenna-Abastumani School on Plasma Astrophysics*, vol. 1, pp. 165–171, ESA SP-285, 1988.

Gurgiolo, C., H. K. Wong, and D. Winske, Low and high frequency waves generated by gyrophase bunched ions at oblique shocks, *Geophys. Res. Lett.*, *20*, 783–786, 1993.

Krasnoselskikh, V. V., M. A. Balikhin, D. Mourenas, A. A. Petrukovich, L. J. C. Woolliscroft, A. K. Pardaens, H. S. Alleyne, M. N. Nozdrachev, and S. I. Klimov, Low frequency plasma turbulence in the front of the supercritical quasiperpendicular collisionless shocks, preprint, 1994.

Krauss-Varban, D., F. G. Pantellini, and D. Burgess, Electron dynamics and whistler waves at quasi-perpendicular shocks, *Geophys. Res. Lett.*, *26*, 2091–2094, 1995.

Matthews, A., Current advance method and cyclic leapfrog for 2D multispecies hybrid plasma simulations, *J. Comput. Phys.*, *112*, 102–116, 1994.

Orlowski, D. S., and C. T. Russell, Ulf waves upstream of the Venus bow shock: Properties of one-Hertz waves, *J. Geophys. Res.*, *96*, 11,271–11,282, 1991.

Orlowski, D. S., C. T. Russell, D. Kraus-Varban, and N. Omidi, On the source of upstream whistlers in the venus foreshock, in *COSPAR Colloquia, Plasma environments of non-magnetic Planets*, vol. 4, edited by T. I. Gombosi, pp. 217–227, Pergamon Press, New York, 1994.

Orlowski, D. S., C. T. Russell, D. Kraus-Varban, N. Omidi, and M. F. Thomsen, Propagation and damping of broadband upstream whistlers, *Adv. Space Res.*, *15*, 85–92, 1995.

Rönmark, K., WHAMP-waves in homogeneous, anisotropic, multicomponent plasmas, *Tech. Rep. 179*, Kiruna Geophysical Institute, 1982.

Thomas, V. A., Dimensionality effects in hybrid simulations of high Mach number collisionless perpendicular shocks, *J. Geophys. Res.*, *94*, 12,009–12,014, 1989.

Tokar, R. L., and D. A. Gurnett, The propagation and growth of whistler mode waves generated by electron beams in the Earth's bow shock, *J. Geophys. Res.*, *90*, 105–114, 1985.

Winske, D., and K. B. Quest, Magnetic field and density fluctuations at perpendicular supercritical shocks, *J. Geophys. Res.*, *93*, 9681–9693, 1988.

Wong, H. K., and M. L. Goldstein, Proton beam generation of oblique whistler waves, *J. Geophys. Res.*, *93*, 4110–4114, 1988.

P. Hellinger, Institute of Atmospheric Physics, Prague, CZ 14131

A. Mangeney, DESPA, Observatory of Paris, Meudon, FR 92190

A. Matthews, Department of Physics, University of Natal, Durban, SA 4001

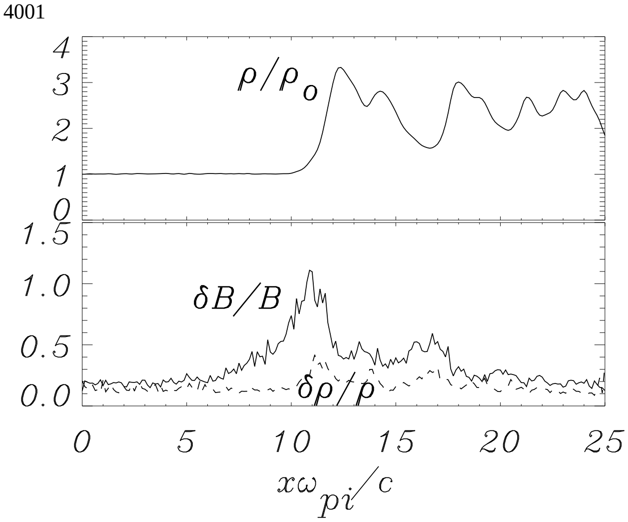

Figure 2. Mean density profile (top panel) and relative magnetic field and density fluctuations (bottom panel).

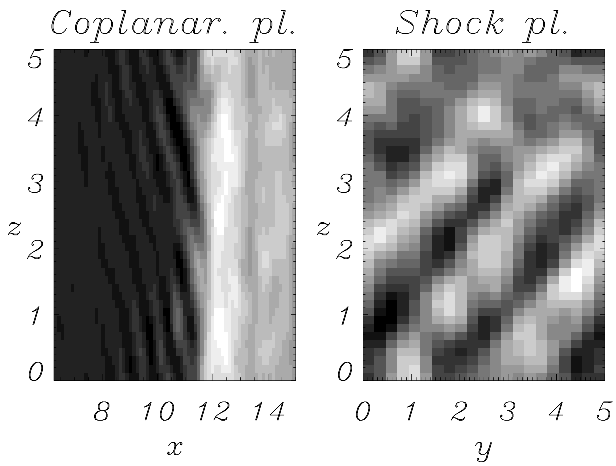

Figure 3. Two-dimensional cuts of B_z in the coplanarity plane and in the shock plane. Distances are in units of c/ω_{pi}.

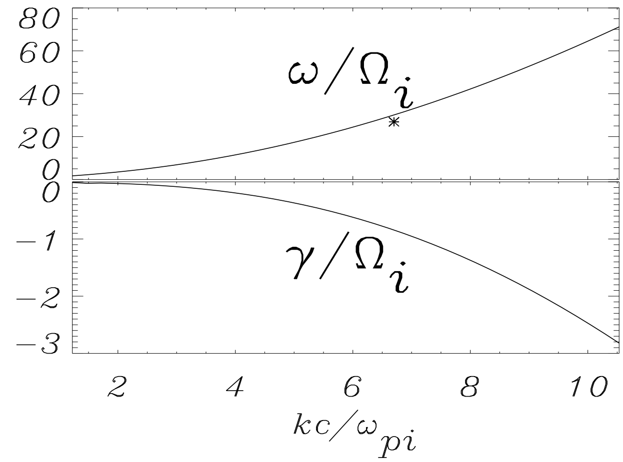

Figure 4. Real frequency ω and damping rate γ for the whistler mode with $\theta_{kB} = 131^{\circ}$ in a plasma with Maxwellian proton and electron distributions, $\beta_p = \beta_e = 0.5$. The asterisk in the top panel denotes the simulation result.